

## A DESIGN METHOD OF A DYNAMIC COMPENSATOR OF CONICAL MODES FOR MAGNETIC BEARINGS OF A RIGID SPINNING ROTOR

Chikara MURAKAMI

Faculty of Aerospace Engineering, Tokyo Metropolitan Institute of Technology,  
 6-6 Asahigaoka, Hino-shi, Tokyo 191, Japan

### Abstract

A design method of a dynamic compensator for magnetic bearings levitating a spinning rigid rotor is proposed. The basic control concept is to move not the rotor directly but the angular momentum vector. The control strategy is to move the angular momentum vector to the spinning axis for nutation suppression and to move the vector to the central position of the stator for precession suppression. It is necessary to estimate the angular momentum vector. An easy estimation method is presented here without using complex observer system or rate signals. A block diagram of the total system including the dynamic compensator clarifies physical meaning of the cross-feedback. Approximate analytic eigen values of the total system are obtained using complex number variables. Several simulation examples are given, showing validity of the approximate analytic solutions.

### Introduction

There are two conical modes in whirling motion of rigid spinning bodies supported by active magnetic bearings. They are a low frequency (backward) mode and a high frequency (forward) one. The control strategy is to move the angular momentum vector,  $H$ , of the rotor to the central axis of the stator or desired rotor position for suppression of the former mode and to the spinning axis for suppression of the latter one. Therefore, it is necessary to obtain signals of  $H$  position or rate signals of tilting angles of the rotor to control any mode. In this paper, an easy method for estimation of  $H$  without using complex observer system or rate signals is proposed, and a simple method for construction of a dynamic compensator for suppression of both modes from a standpoint of physical meaning are presented. Approximate analytical eigen values of the total system including the dynamic compensator are also presented. Simulation examples verify effectiveness of above-mentioned method. These concepts may suggest some new control methods of flexible spinning rotors.

### 1. Outline of conical motions

$H$  of the axi-symmetrical spinning rotor (the rotor, in the following) is governed by the following simple equation:

$$dH/dt = T \quad (1)$$

where  $T$  is external or control torques. Therefore,  $H$  is easily controllable by  $T$ . However,  $H$  is invisible, instead, position of the rotor or the spinning axis,  $S$ , is visible and sensed

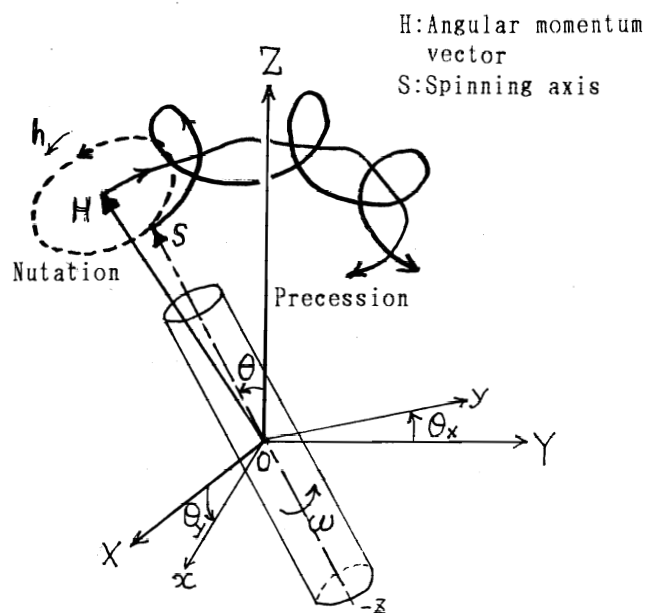


Fig. 1 Nutation, precession, coordinate system and notation

by gap sensors. Generally, in magnetic bearings,  $T$  contains at least restoring torque which is negative and proportional to small tilt angle,  $\theta$ , of  $S$ , i.e.  $T = -K\theta$ , where  $K$  is restoring coefficient. When  $H$  is near to  $S$ , direction of the restoring torque is clockwise as seen in Figure 1. In the field of satellite control, motion of  $H$  is called precession, whereas motion of  $S$  around  $H$  is called nutation. Generally,  $S$  draws a cone or a circle when we see the motion from headside of  $H$ .

The cone angle  $\nu$  is decided by  $S$  and  $H$  at each instant, where only  $H$  is directly moved by  $T$ . Rotational speed of  $S$  around  $H$  or nutational angular velocity seen from stator-side,  $h$ , is independent of magnitude of  $\nu$  when  $\nu$  is small.  $h$  and  $\nu$  are expressed as follows:

$$h = \sigma \omega \quad (2)$$

where  $\sigma$  is moment of inertia ratio ( $I_s/I_a$ ) of the rotor with spinning speed  $\omega$  (Ref. [1]), and

$$\nu = \tan^{-1}(I_a \theta' / I_s \omega) \approx \theta' / h \quad (3)$$

where  $'$  means 1st order time derivative. Note that nutation is always anti-clockwise, whereas precession is clockwise in case of magnetic bearings, anti-clockwise in case of a top on the ground where restoring torque is negative.

From above-mentioned characteristics, the control strategy is easily derived:

- (1) For suppression of nutation,  $H$  should be moved to  $S$ .
- (2) For suppression of precession,  $H$  should be moved to the central position.

In order to do these, we must know  $H$  position.

## 2. Equations of motion

Let  $O$ - $XYZ$  be an inertia coordinate system whose origin  $O$  coincides with center of mass of the rotor, and  $Z$ -axis is parallel to the central axis of the stator. For convenience of expressing the spinning axis  $S$ , let's adopt a moving but non-spinning coordinate system,  $o$ - $xyz$ , whose origin  $o$  and  $z$ -axis coincide with center of mass and spinning axis  $S$  of the rotor, respectively. Of course,  $x$  and  $y$  axes are not fixed to the rotor but always near the  $X$  and  $Y$  axes, respectively (see Fig. 1).

Small tilt angle  $\theta$  is decomposed to  $\theta_x$  and  $\theta_y$ , and expressed as a complex number:

$$\underline{\theta} = \theta_x + i \theta_y \quad (i = \sqrt{-1}) \quad (4)$$

In the following, complex numbers are expressed by underlined characters, and  $''$  means 2nd order time derivatives. Using Eq. (4), Eq. (1) becomes

$$\underline{\theta}'' - i h \underline{\theta}' + k \underline{\theta} = \underline{T} \quad (5)$$

where  $k = K/I_a$  and  $\underline{T} = (T_x + iT_y)/I_a$ . In case of high speed and  $\underline{T} = 0$ , we get two approximate eigen values:

- +  $i h$  (high freq. or N mode)
- $i k/h$  (low freq. or P mode)

$N$  and  $P$  stand for nutation and precession, respectively. Note that, though, motions of  $H$  include both modes, they comprize almost  $P$  mode alone (Ref. [1]).

In order to visualize attitude of  $S$  and  $H$ ,

we define a complex number plane  $Z=1$  on which real and imaginary axes are parallel to  $X$  and  $Y$  axes, respectively.  $\underline{S}$  and  $\underline{H}$  are the positions where they cross the plane. Then  $\underline{S}$  is expressed as:

$$\underline{S} = \theta_y - i \theta_x = -i \underline{\theta} \quad (6)$$

Using Eq. (3), we get

$$\underline{H} - \underline{S} = \underline{\theta}' / h \quad (7)$$

## 3. Estimation of $H$

We can estimate approximate  $\underline{H}$ ,  $\underline{H}_e$ , from  $\underline{S}$  using low pass filter (LPF) by eliminating high frequency mode,  $N$  mode. In this paper, only a first order LPF is used. Its transfer function  $F$ , whose time constant is  $\tau$ , is:

$$F = (1 + \tau s)^{-1} \quad (8)$$

At first, operate  $F$  to  $\underline{S}_s$ , a Laplace transformed variable of  $\underline{S}$ . Here, we choose the breaking frequency,  $1/\tau$ , as follows:

$$k/h < 1/\tau \ll h \quad (9)$$

Phase lag angle  $\alpha$  of LPF at  $P$  mode is

$$\alpha = \tan^{-1}(\tau k/h) \quad (10)$$

Using  $\alpha$ , we can get more accurate  $\underline{H}_e$ , whose Laplace transformed value is  $\underline{H}_{es}$ , by clockwise rotation by  $\alpha$ :

$$\underline{H}_{es} = e^{-i\alpha} F \underline{S}_s \quad (11)$$

Sometimes, gain correction may be required.

## 4. Feedback torque for stabilization

Required Laplace transformed feedback torque divided by  $I_a$ ,  $\underline{T}_s$ , for suppressing two modes is expressed as follows:

$$\begin{aligned} \underline{T}_s &= -K_p \underline{H}_{es} - K_n (\underline{H}_{es} - \underline{S}_s) \\ &= -(K_p + K_n) \underline{H}_{es} + K_n \underline{S}_s \\ &= -K_{pn} \underline{H}_{es} + K_n \underline{S}_s \end{aligned} \quad (12)$$

$$\text{where } K_{pn} = K_p + K_n \quad (13)$$

$K_{pn}$  may include gain correction for  $\underline{H}_{es}$  estimation.  $K_p$  and  $K_n$  are feedback gain for  $P$  and  $N$  modes suppression, respectively. Using Eq. (6) and Eq. (11), Eq. (13) becomes:

$$\underline{T}_s = (-K_{pn} e^{-i\alpha} F + K_n) (-i \underline{\theta}_s) \quad (14)$$

where  $\underline{\theta}_s$  is Laplace transformed variable of  $\underline{\theta}$ . Clearly, Eq. (14) expresses the inter-axis cross coupling feedback (or simply, cross feedback).

5. Compensated system and eigen values

Through Laplace transformation of Eq. (5), and using Eq. (14), we get the following 3rd order characteristic equation :

$$\tau s^3 + (1 - i\tau h)s^2 + [\tau k + i(\tau K_n - h)]s + k - K_n \sin \alpha + i(K_n - K_p \cos \alpha) = 0 \quad (15)$$

Under the condition of Ineq. (9) and small region of  $K_n$  and  $K_p$ , approximate eigen values of three modes,  $\lambda_n$ ,  $\lambda_p$  and  $\lambda_\tau$  ( $\tau$  mode) are :

$$\lambda_n = -(K_n/h) + ih(1 - K_n/(\tau h^2)) \quad (16)$$

$$\lambda_p = -(K_p + ik)/(h - \tau K_n) \quad (17)$$

$$\lambda_\tau = -(1/\tau) + ((K_p + K_n)/h) - (\tau K_p K_n/h^2) + i[\tau k(K_p + K_n)/h^2] \quad (18)$$

From Eqs. (16) and (17), it is clear that the compensation or the cross feedback gives N and P mode dampings which are proportional to  $K_n$  and  $K_p$ , respectively. And these results show validity of control law, Eq. (12), derived from standpoint of dynamics. Eqs. (17) and (18) show that restoring coefficient,  $k$ , has no effect on damping but effects for increasing vibratory frequencies, though indispensable to stability at low rotation speed. In Eq. (17), it is required for stability that denominator be positive :

$$h > \tau K_n \quad (19)$$

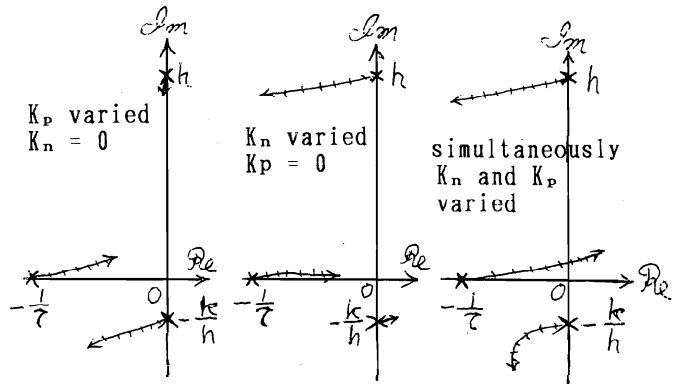


Fig. 2 Root loci of compensated system

Inequality (19) gives some restrictions on  $\tau$  and  $K_n$  at low rotation speed. The second term of Eq. (18) shows that too large  $K_n$  and  $K_p$  may introduce instability in  $\tau$  mode at low rotation speed. In any case, we should pay attentions to variation of rotation speed.

Figure 2 shows root loci where  $K_p$  and/or  $K_n$  increase from zero to some high values in a numerical example shown in the next chapter.

A block diagram of the compensated total system is shown in Fig. 3, where  $F$ ,  $e^{-i\alpha}$  and cross-feedback are described concretely.

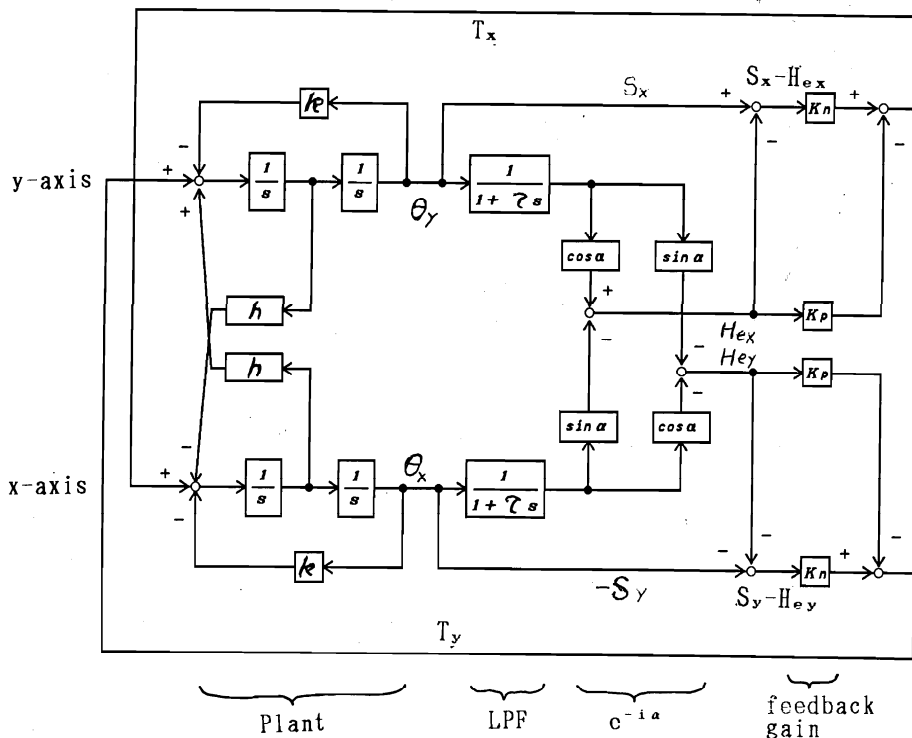


Fig. 3 Block diagram of compensated total system

6. Numerical simulation examples

The following model was used and run by computer:  $\sigma = I_s/I_a = 0.5$ ,  $h = \sigma \omega = 1000$  [rad/s],  $k = 1.51 \times 10^4$  [s<sup>-2</sup>],  $\tau = 2.73$  [ms],  $1/\tau = 366$  [rad/s],  $\alpha = 22.4$  [deg],  $k/h = 151$  [rad/s].

Figure 4 is a case of no control ( $K_p = K_n = 0$ ). Of course, there is neither divergence nor convergence. In addition to loci of S and H, a locus of the signal passed through the LPF is shown by dotted line where some gain reduction is observed and measured value of phase lag angle,  $\alpha$ , is 25 [deg].

Several cases with  $K_p$  and/or  $K_n$  are simulated. Results are the same as Fig. 2.

In Fig. 5, two gains have non-zero values ( $K_n = K_p = 1.58 \times 10^5$  [s<sup>-2</sup>]). Both modes decay rapidly. At the beginning of the H motion, H goes outside. This comes from a mistake where zero was given as the initial value of LPF, indicating  $H_e$  is at the origin, therefore, H was moved to S direction.

Effects of  $\alpha$  correction is difficult to estimate by analytical solution. Here, root loci of the above-mentioned model when  $\alpha$  is varied are shown in Figs. 6, 7 and 8. Effect on P mode is shown in Fig. 6 where the nominal value is on the best position. Effect on N mode is shown in Fig. 7 where the nominal value is on not so good position, but the negative real part is almost the same as P mode, therefore, it is unnecessary to change. Figure 8 is the case of  $\tau$  mode, where the nominal value position has quite large magnitude of negative real part. Again, therefore, it is needless to change. In this example,  $\alpha$  correction brings about 30% increase of damping of both N and P modes.

It is interesting to note that phase adjustment can be attained by geometrical rotation of signals on the rotating plane.

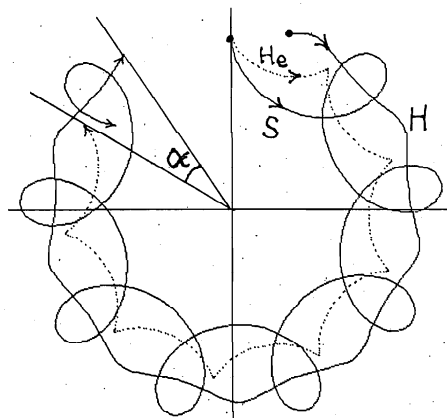


Fig. 4 Loci of S, H and  $H_e$  of uncontrolled system

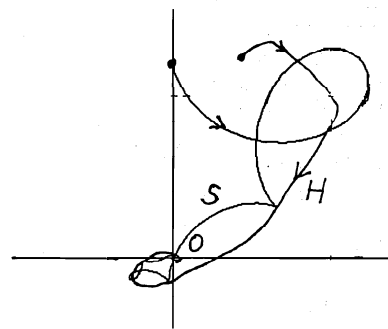


Fig. 5 Loci of S and H of controlled system

Reference

- [1] "Magnetic Bearings" (Proceedings of 1st international symposium on magnetic bearings) Springer Verlag, 1989, pp. 311~318.

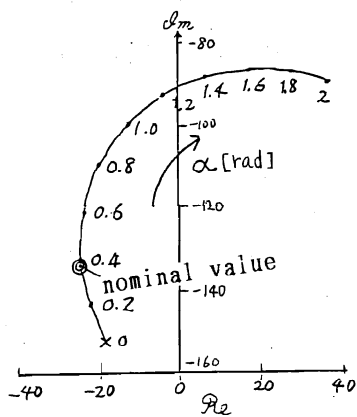


Fig. 6 Root locus of P mode

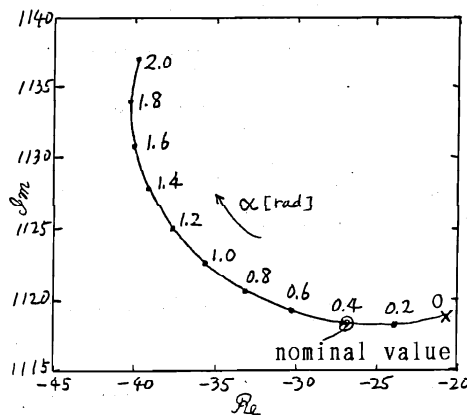


Fig. 7 Root locus of N mode

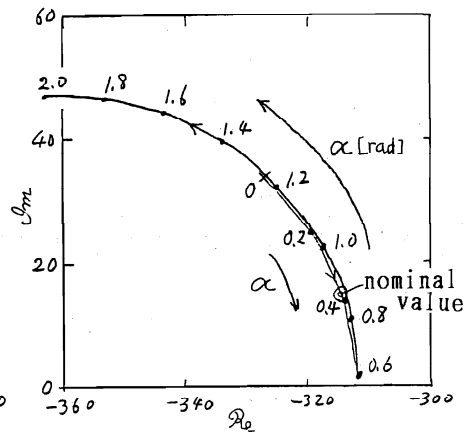


Fig. 8 Root locus of  $\tau$  mode